JOURNAL OF VIROLOGY, Sept. 1994, p. 5384–5394
0022-538X/94/$04.00+0

Vol. 68, No. 9

Phenotype of the Herpes Simplex Virus Type 1 Protease Substrate ICP35 Mutant Virus

LINDA MATUSICK-KUMAR,[1] WARREN HURLBURT,[1] STEVEN P. WEINHEIMER,[1] WILLIAM W. NEWCOMB,[2] JAY C. BROWN,[2] AND MIN GAO[1]*

Department of Virology, Bristol-Myers Squibb Pharmaceutical Research Institute, Princeton, New Jersey 08543-4000,[1] and Department of Microbiology and Cancer Center, University of Virginia Health Science Center, Charlottesville, Virginia 22908[2]

Received 4 April 1994/Accepted 25 May 1994

The herpes simplex virus type 1 ICP35 assembly protein is involved in the formation of viral capsids. ICP35 is encoded by the UL26.5 gene and is specifically processed by the herpes simplex virus type 1 protease encoded by the UL26 gene. To better understand the functions of ICP35 in infected cells, we have isolated and characterized an ICP35 mutant virus, Δ*ICP35*. The mutant virus was propagated in complementing 35J cells, which express wild-type ICP35. Phenotypic analysis of Δ*ICP35* shows that (i) mutant virus growth in Vero cells was severely restricted, although small amounts of progeny virus were produced; (ii) full-length ICP35 protein was not produced, although autoproteolysis of the protease still occurred in mutant-infected nonpermissive cells; (iii) viral DNA replication of the mutant proceeded at wild-type levels, but only a very small portion of the replicated DNA was processed to unit length and encapsidated; (iv) capsid structures were observed in Δ*ICP35*-infected Vero cells by electron microscopy and by sucrose sedimentation analysis; (v) assembly of VP5 into hexons of the capsids was conformationally altered; and (vi) ICP35 has a novel function which is involved in the nuclear transport of VP5.

The herpes simplex virus type 1 (HSV-1) DNA is synthesized as large concatemers, processed into unit-length molecules, and encapsidated into capsids in the infected-cell nucleus (16, 19). The viral capsid is an icosahedral protein shell consisting of 162 capsomers, 150 hexons, and 12 pentons (47). Three types of capsids, designated A, B, and C, can be separated by sucrose gradient sedimentation of nuclear lysates from HSV-1-infected cells (12). The C capsids contain the viral genome and are able to mature into infectious virions. The A capsids are thought to result from aborted assembly; they have the same protein content as C capsids but lack DNA (12, 29). The B capsids also lack DNA but are thought to be intermediates in capsid assembly (29, 30), because they are distinguished by the presence of large amounts of the viral assembly protein, ICP35 (VP22a) (1, 3, 25).

Detailed studies of B capsids have shown that they are composed of at least seven proteins, VP5, VP19c, Na (VP21), ICP35 (VP22a), VP23, N_0 (VP24), and VP26 (1, 13, 27, 38, 42). The major capsid protein, VP5, which has an apparent molecular mass of 150 kDa, accounts for about 70% of the mass of the capsid surface shell (38, 42). Genetic analysis of a VP5 deletion mutant virus demonstrated that no capsid structures were obtained in the absence of VP5 and therefore that VP5 is essential for viral growth (7). It has been shown that 960 copies of VP5 are present in each capsid and that it is the structural subunit of the capsomers, both the hexons and the pentons (27). It appears that VP5 holds different conformations in the hexons and the pentons, because a panel of monoclonal antibodies (MAb) specific for VP5 can discriminate the hexons from the pentons (41). In addition to VP5, there are approximately 1,100 copies of ICP35 but only approximately 100 of N_0 and Nb per capsid (26, 27). The remaining capsid proteins are present at approximately 400 to 1,000 copies per capsid (26, 27).

Genetic and functional analyses clearly demonstrated that the HSV-1 genome encodes a protease, designated Pra, responsible for the processing of ICP35 (21–23). Moreover, N_0 and Nb are products of the protease, resulting from autoproteolytic cleavage. Pra is encoded by the UL26 gene, and ICP35 is encoded by the UL26.5 gene. UL26 and UL26.5 genes have their own promoters and are transcribed as two mRNAs which coterminate at the 3′ end but have different 5′ ends (15, 20, 24). The UL26 gene encodes 635 amino acids; UL26.5 encodes 329 amino acids initiating at a methionine which corresponds to residue 307 of the UL26 open reading frame (20). Therefore, ICP35 shares sequence identity with the C-terminal 329 amino acids of Pra. Antibodies against ICP35 detected the protease in addition to unprocessed and processed forms of ICP35 (ICP35 c,d and e,f, respectively) (3). A temperature-sensitive (*ts*) mutant, *ts*1201, showed reduced processing of ICP35 c,d to e,f and failed to package viral DNA at the nonpermissive temperature (33, 34, 36). However, the *ts* lesion was mapped in the UL26 gene, upstream of the UL26.5 gene encoding ICP35 (33). Pra expressed in both eukayotic cells and *Escherichia coli* has been demonstrated to specifically cleave a site near the C terminus of ICP35 and Pra (21–23). A second autoproteolysis site was first identified in the N terminus of the homologous protease gene product of cytomegalovirus, and cleavage at this site releases the catalytic domain of the protease (45). For HSV-1, the N-terminal autoproteolysis occurs between Ala-247 and Ser-248 of Pra and generates Na and the catalytic domain N_0 (VP24) (Fig. 1A) (6, 8, 21–23, 31, 43). An additional autocleavage site was identified in the catalytic domain of the cytomegalovirus protease but not in the HSV-1 protease (2, 44).

We recently reported the isolation and characterization of the HSV-1 protease deletion mutant virus *m*100 (9). In *m*100-infected Vero cells, normal amounts of ICP35 c,d were produced but failed to be processed into e,f. In addition, assembly

* Corresponding author. Mailing address: Department of Virology, Bristol-Myers Squibb Pharmaceutical Research Institute, P.O. Box 4000, Princeton, NJ 08543-4000. Phone: (609) 252-6467. Fax: (609) 252-6058.

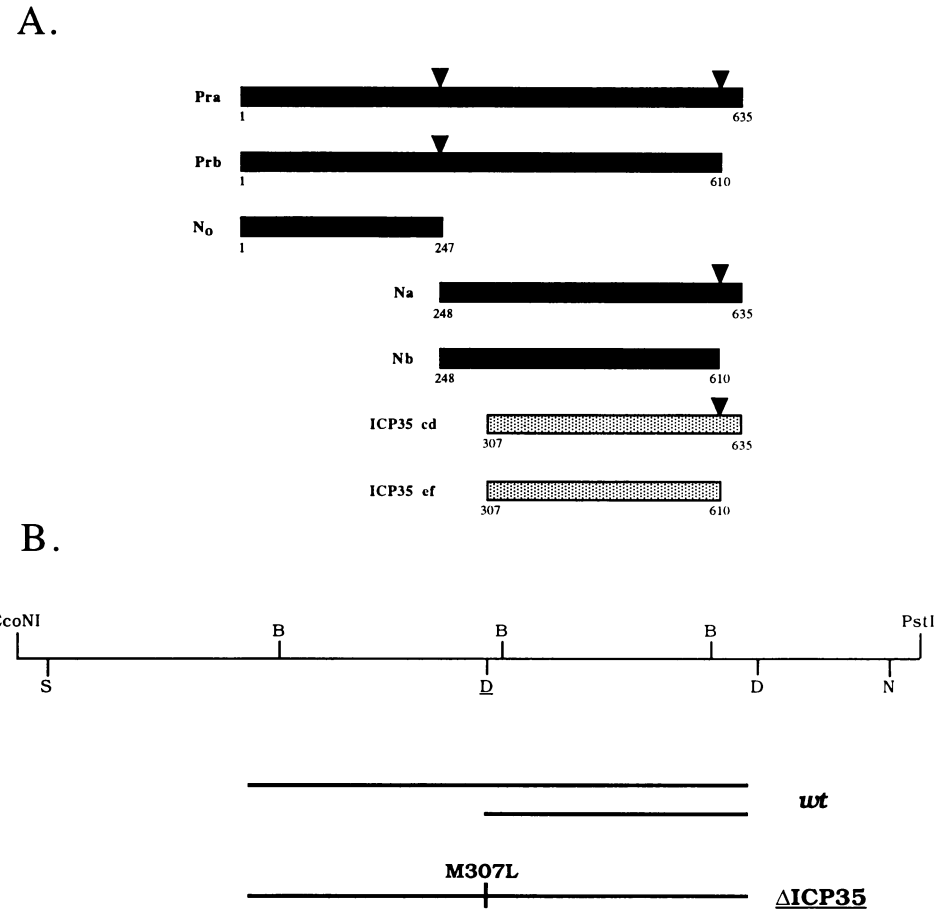

FIG. 1. (A) Polypeptide products of UL26 and UL26.5 open reading frames. The HSV-1 protease (Pra), substrate (ICP35 c,d), and cleavage products Prb, N_0 (VP24), Na, Nb (VP21), and ICP35 e,f (VP22a) are described in the text. The sites of cleavage of Pra and ICP35 c,d are indicated by arrows. The UL26 amino acid numbers of N and C termini of each protein are indicated. (B) The UL26 and UL26.5 open reading frames of HSV-1 wt and mutant Δ*ICP35* genomes. Plasmid pRB4057 containing the UL26 and UL26.5 genes (*Eco*NI-*Pst*I fragment) was kindly provided by B. Roizman (20). Restriction enzyme sites are shown on the top line: B, *Bam*HI; S, *Sph*I; N, *Nhe*I; D, *Dra*I; D, an extra *Dra*I site generated only in plasmid pM307L and the mutant Δ*ICP35* genome.

of VP5 into the hexons of capsids was conformationally altered in mutant-infected cells, although formation of the pentons appeared to be normal. It is still unclear whether the processing of ICP35 is essential for viral growth. Because ICP35 is present in large amounts in B capsids and absent from mature virions, it has been postulated that ICP35 is analogous to the scaffold protein of double-stranded DNA bacteriophage (5, 26). Since no ICP35 mutant virus has been isolated, the precise role of ICP35 during the viral life cycle is basically unknown.

In this report, we describe the isolation and characterization of an ICP35 mutant virus. Our results indicate that although ICP35 plays an important role during capsid assembly and maturation of the virion, it is not absolutely essential for viral growth.

MATERIALS AND METHODS

Cells and viruses. Vero cells were grown and maintained as described previously (17). The growth medium for the neomycin-resistant cell lines BMS-MG22, X4 (9), and 35J (see below) included 250 μg of the antibiotic G418 per ml.

The HSV-1 wild-type (wt) strain KOS1.1 and HSV-2 wt strain 186 were propagated and assayed as described previously (17, 18). The mutant virus Δ*ICP35* was grown in the ICP35-expressing 35J cell line.

Plasmids. Plasmid pRB4057 of HSV-1 F was kindly provided by B. Roizman, University of Chicago (Fig. 1B) (21). The construction of pM307L was described previously (9); this plasmid was derived from pRB4057 by changing CCCAT GAAC (Pro-Met-Asp) to CCTTTAAAC (Pro-Leu-Asp) by standard PCR techniques. Therefore, pM307L encodes the HSV-1 protease with the Met-to-Leu change at residue 307. Since residue 307 (Met) of the protease is also the start codon for ICP35, the mutation should eliminate the synthesis of full-length ICP35 molecules. In addition to the desired base substitution for the M307L change, the silent mutation generated an extra *Dra*I site. Mutations in pM307L were confirmed by DNA sequencing. pUCICP35 was constructed by ligating the 2-kb *Hpa*I-*Hin*dIII fragment of pRB4057 into the *Sma*I-*Hin*dIII sites of pUC18. Thus, pUCICP35 encodes ICP35 expressed from its own promoter.

Isolation of mutant Δ*ICP35* virus. An ICP35 mutant virus was constructed by cotransfection of X4 cells with infectious KOS1.1 DNA and plasmid pM307L. The progeny viruses from the marker transfer were tested for their ability to grow in X4 and Vero cells. One of the more than 200 viruses tested could

TABLE 1. Titers of mutant Δ*ICP35* virus generated in 35J cells

Virus	Titer (PFU/ml)[a] in:		Titer ratio (Vero/35J)
	Vero cells	35J cells	
wt	9.8×10^8	7.0×10^8	1.4
Δ*ICP35*	$<2 \times 10^4$[b]	9.6×10^8	$<2.1 \times 10^{-5}$
	1.0×10^7[c]		

[a] Titers of viral stocks were determined by plaque assay on the cell lines indicated, and plaques were counted 2 days p.i.
[b] Large plaques.
[c] Very small plaques. Because of size, numbers may not be accurate.

grow in X4 cells but was unable to grow well in Vero cells. This virus was designated Δ*ICP35*.

Isolation of ICP35-expressing cell lines. Vero cells were transformed with plasmid pUCICP35 and pSVneo as described previously (10, 40). G418-resistant colonies were grown into cultures and screened for their ability to complement the growth of Δ*ICP35*. The cell clone 35J, derived from a culture transfected with plasmid pUCICP35, yielded the highest level of complementation and lowest level of revertants (Table 1). X4 cells, derived from a culture transfected with plasmid pRB4057, yielded lower levels of complementation of Δ*ICP35* (results not shown).

Analysis of viral DNA and proteins. Viral DNA for marker transfer was prepared as described previously (10). For Southern blot analysis, total and encapsidated (DNase I-treated) DNAs were prepared from Vero or 35J cells infected with wt or Δ*ICP35* virus at a multiplicity of infection (MOI) of 10 PFU per cell and analyzed essentially as described by Shao et al. (39). To quantitate data, the intensity of radioactivity hybridizing to the *Bam*HI S fragments in DNase I-treated samples was scanned and the number of counts per minute to the *Bam*HI S fragment in Δ*ICP35*-infected Vero cells in the presence of phosphonoacetate (400 μg/ml) was subtracted from the values obtained from the infected-cell DNA in the absence of phosphonoacetate.

For Western immunoblot analysis of infected-cell lysates, cell monolayer cultures were infected with KOS1.1 or Δ*ICP35* virus at an MOI of 10 and harvested as indicated in Results. Sodium dodecyl sulfate-polyacrylamide gel electrophoresis (SDS-PAGE) was performed as described previously (10, 43). The proteins were transferred to nitrocellulose filters by electrophoresis. Detection of immune complexes on blots by a Western blot procedure involving a color reaction for the alkaline phosphatase activity was conducted as specified by the manufacturer (Promega Biotec, Madison, Wis.). The anti-ICP35 MAb MCA406 (1:1,000 dilution; Serotec, Oxford, England) was used to detect ICP35 protease-related products Pra, Prb, Na, and Nb. A rabbit polyclonal antiserum (1:200 dilution) raised against a polypeptide containing the C-terminal 25 amino acids was used to determine Pra, Na, and polypeptides containing C-terminal cleavage products, and N_0 was detected by a polyclonal antiserum (N-term rAb; 1:200 dilution) raised against N_0 (43).

Electron microscopy. Infected cells to be examined in the electron microscope were centrifuged into a small (0.3-ml) pellet, fixed with 2.5% glutaraldehyde in 0.1 M phosphate buffer (pH 7.4) for 24 h at 4°C, and postfixed with 2% OSO_4 for 1 h at 24°C. Pellets were then washed in water, dehydrated in graded concentrations of acetone, embedded in Epon 812, and cut into sections (~70 nm thick) with a Richert Ultracut E ultramicrotome. Sections were stained with a saturated solution of uranyl acetate in methanol for 20 min at 60°C and then with 0.25% lead citrate for 2 min at 24°C and examined in a JEOL 100CX transmission electron microscope operated at 80 keV.

Sucrose gradient sedimentation. Vero cells were infected with 10 PFU of virus per cell for 16 h, and nuclei were prepared as described by Shao et al. (39). The nuclei were suspended in 0.5 ml of buffer containing 10 mM Tris (pH 7.5), 1 mM EDTA, and 1 mM dithiothreitol with 1% Triton X-100 and 10% glycerol and lysed by sonication. After clarification by low-speed centrifugation, nuclear lysates were layered on 20 to 50% sucrose gradients as described by Desai et al. (7) and centrifuged at 25,000 rpm for 60 min in a Beckman SW41 rotor.

Indirect immunofluorescence. Indirect immunofluorescence was performed as described previously (10, 35). The anti-ICP35 MAb MCA406 (1:100 dilution); anti-VP5 MAb 8F5 (1:40 dilution [41]), 5C (1:40 [41]), or MAb 3B (1:75 dilution [41]); and fluorescein-conjugated goat anti-mouse antibody (1:150 dilution) were used.

RESULTS

Isolation of ICP35 complementing cell lines and the mutant Δ*ICP35* virus. Studies were initiated to determine the role of ICP35 during capsid assembly by characterizing HSV-1 ICP35 mutant viruses. We recently reported isolation of a cell line (X4), derived from a culture transfected with plasmid pRB4057 encoding both protease and ICP35. Since X4 cells could complement the growth of the HSV-1 protease mutant *m*100 (9), we expected that it would also serve as an efficient host for the isolation of ICP35 mutant viruses.

The ICP35 mutant plasmid, pM307L, was constructed by changing the ICP35 initiation codon ATG (Met) to TTA (Leu). Thus, pM307L encodes the HSV-1 protease with a Met-to-Leu change at residue 307, which should eliminate the synthesis of intact ICP35 (Fig. 1B). Recent studies demonstrated that this mutant HSV-1 protease retained all the functional activity of wt protease (9). The mutation in pM307L was transferred into the wt HSV-1 KOS1.1 genome by marker transfer. Over 200 plaque isolates resulting from cotransfection of X4 cells were tested for their ability to grow on X4 cells relative to Vero cells. One isolate formed small plaques on X4 but formed extremely small plaques on Vero cells.

We then used this putative ICP35 mutant to screen cell lines derived from cultures transfected with a plasmid pUCICP35 encoding only wt ICP35. One cell line, 35J, yielded the highest level of complementation (Table 1). X4 cells yielded a lower level of complementation and smaller plaques than 35J cells did (results not shown). Like X4 cells, 35J cells were derived from a single cell colony. The putative ICP35 mutant virus was plaque purified three times on 35J cells and designated as Δ*ICP35*.

Analysis of viral mutant Δ*ICP35*. To ensure that the engineered mutation had been introduced into the recombinant virus, we analyzed the mutant genome by Southern blotting (Fig. 2). Total viral DNA isolated from Δ*ICP35*-infected V35J cells was digested with *Bam*HI or *Dra*I or both and hybridized with plasmid pRB4057, containing the wt UL26 and UL26.5 genes as a probe. wt and Δ*ICP35* viral DNAs contained four identical hybridizing fragments: *Bam*HI-G (7.8 kb), *Bam*HI-U (2.3 kb), *Bam*HI-d′ (863 bp), and *Bam*HI-e′ (797 bp) (Fig. 2, lanes 1 and 3). Two overlapping *Dra*I fragments were observed in *Dra*I-digested wt DNA (31 and 25 kb [lane 2]). In contrast, the Δ*ICP35* DNA generated a new *Dra*I fragment of 1.0 kb because of the engineered mutation (lane 4). This was further confirmed by *Bam*HI-*Dra*I double digestions (compare lanes 5

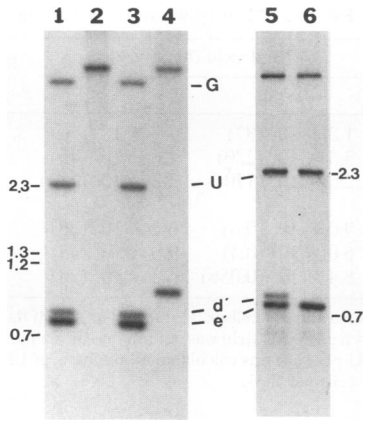

FIG. 2. Southern blot analysis of KOS1.1 and Δ*ICP35* genomes. Total DNAs from wt KOS1.1-infected cells (lanes 1, 2, and 5) or Δ*ICP35*-infected cells (lanes 3, 4, and 6) were digested with *Bam*HI, *Dra*I, and *Bam*HI-*Dra*I, respectively. Digested DNAs were separated on a 0.8% agarose gel, blotted onto a nylon membrane, and hybridized to ^{32}P-labeled plasmid pRB4057 (Fig. 1B). The locations of molecular size markers are shown at the left (lanes 1 to 4) and right (lanes 5 and 6).

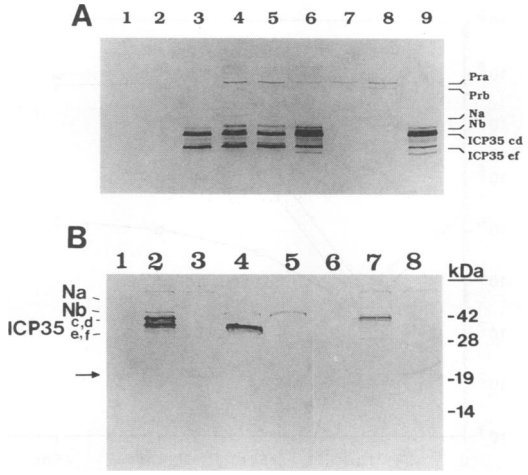

FIG. 3. Western blot analysis of HSV-1 protease-related polypeptides in wt- or Δ*ICP35*-infected cells. (A) Vero (lanes 2, 4, and 7), BMS-MG22 (lanes 5 and 8), and 35J cells (lanes 1, 3, 6, and 9) were mock infected (lane 1) or infected with HSV-2 (lanes 2 and 3), KOS1.1 (lanes 4 to 6), or Δ*ICP35* (lanes 7 to 9). Total proteins were prepared at 9 h p.i., separated by SDS-PAGE (12.5% polyacrylamide), and transferred to a nitrocellulose filter. The filter was probed with a MAb MCA406 specific for ICP35. (B) Vero cells were mock infected (lanes 1 and 6) or infected with wt (lanes 2 and 7) or Δ*ICP35* (lanes 3 and 8) virus. Total proteins were prepared at 9 h p.i., separated by SDS-PAGE (15% polyacrylamide), and transferred to nitrocellulose filters. Samples from the sucrose gradient (see Fig. 7) fraction 12 of wt-infected Vero nuclear lysate (lane 4) and fraction 10 of Δ*ICP35*-infected nuclear lysate (lane 5) were used as controls. The filters were probed with MAb MCA406 specific for ICP35 (lanes 1 through 5) and a polyclonal antiserum specific for the C-terminal 25 amino acids of the protease and ICP35 (lanes 6 through 8).

and 6); the *Bam*HI d′ fragment (863 bp) of Δ*ICP35* DNA was cleaved at the extra *Dra*I site at codon 307 to generate a new 801-bp fragment (lane 6). These results demonstrate that the intended mutation was successfully introduced into the recombinant genome.

Phenotype of the mutant. (i) Protease-related proteins expressed by Δ*ICP35*. The viral mutant Δ*ICP35* was analyzed for expression of protease-related polypeptides. Vero, BMS-MG22, and 35J cells were either mock infected or infected with virus. Cell extracts were prepared at 9 h postinfection (p.i.), separated by SDS-PAGE, and analyzed by Western blotting (Fig. 3). No ICP35 was detected in mock-infected extracts (Fig. 3A, lane 1), indicating that 35J cells did not express ICP35 constitutively. We were able to examine the expression of ICP35 from 35J cells after HSV-2 infection, since MAb MCA406 recognizes HSV-1 ICP35 but not HSV-2 ICP35 (lanes 2 and 3) (14, 42). The amount of ICP35 produced by 35J cells after HSV-2 infection was comparable to that produced by HSV-1-infected Vero cells (compare lanes 3 and 4), and the processing of ICP35 was most probably due to activity of the HSV-2 protease. BMS-MG22 cells, derived from cultures transformed with plasmid pM307L, expressed only the HSV-1 protease, containing a Met-to-Leu change at residue 307, after infection (9). Normal amounts of the protease (Pra) were produced in Δ*ICP35*-infected Vero and BMS-MG22 cells and were processed into Prb, Na, and Nb, but no ICP35 was detected (lanes 7 and 8, and results not shown). ICP35 c,d was produced from 35J cells and processed into e,f after Δ*ICP35* infection (lane 9).

Our results demonstrate that the mutation in Δ*ICP35* eliminates the synthesis of full-length ICP35. We also examined whether a truncated form of ICP35 is synthesized by initiation from the second Met codon of UL26.5 located 176 residues downstream of M307L. Cell extracts (9 h p.i.) were prepared and analyzed by Western blotting with MAb MCA406 (Fig. 3B, lanes 1 through 5) and a polyclonal antiserum specific for the C-terminal 25 residues of the protease and ICP35 (lanes 6 through 8). Both antibodies recognized a new protein in the mutant-infected cell extract (lanes 3 and 8) that was absent in the wt-infected cell extract (lanes 2 and 7). The apparent molecular mass of this protein is approximately 20 kDa, close to the predicted size of an ICP35 protein initiated from the second AUG of ICP35. The 20-kDa protein appeared to be processed, because the lower-molecular-mass protein could be detected only by MAb MCA406, not by the polyclonal antiserum specific for the C-terminal 25 residues (results not shown). It is noteworthy that the amounts of this 20-kDa protein produced were much lower than those of ICP35 and showed an approximately equal molar ratio with Pra. At present we do not know whether this 20-kDa protein represents an initiated product or a degradation product of the Pra containing an M307L change.

(ii) Growth properties. The growth property of mutant Δ*ICP35* was examined for its ability to form plaques on Vero and 35J cells. As indicated in Table 1, wt virus formed plaques equally well on both cell types. In contrast, Δ*ICP35* gave rise to large plaques only on 35J cells but formed extremely small plaques on Vero cells. No large plaques were observed at the lowest dilution tested (Table 1). Notably, these small plaques on Vero cells often had several rounded cells in their center and usually disappeared 4 to 5 days p.i. The quantitative amount of mutant virus used in this study was determined by using ICP35-expressing 35J cells. Our results demonstrated that there is a growth defect for Δ*ICP35* and that this growth defect can be efficiently complemented by expression of the wt ICP35 from 35J cells.

To more quantitatively assess the growth characteristics of the mutant virus, we carried out a yield experiment. Vero and 35J cells were infected with either wt or Δ*ICP35* at an MOI of

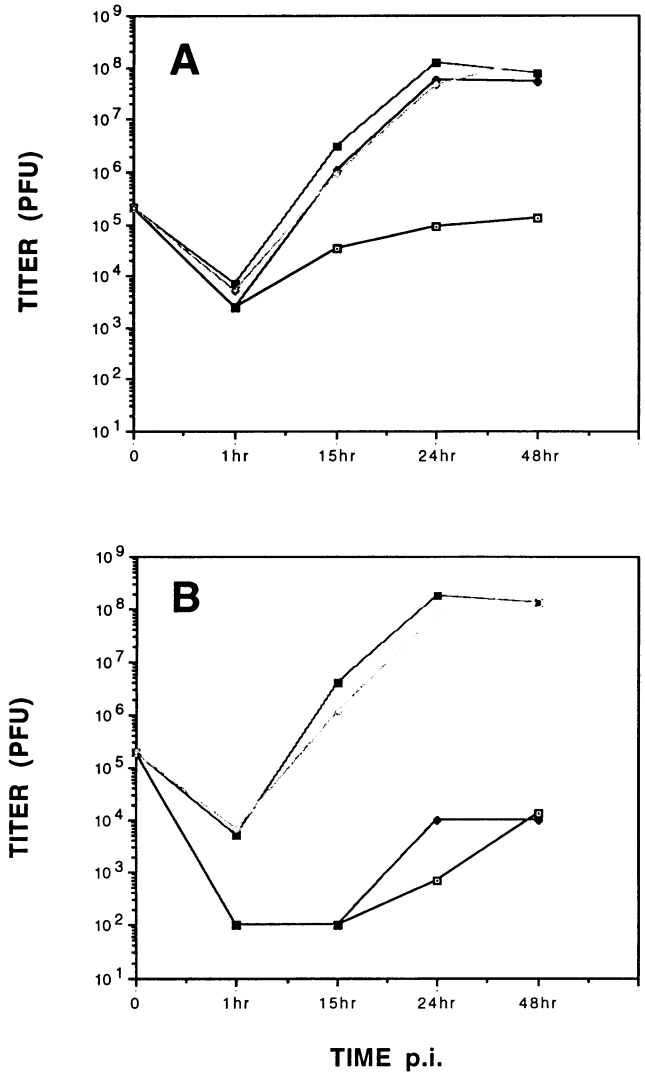

FIG. 4. Single-step growth analysis of wt and mutant Δ*ICP35* in Vero and 35J cells. Cells were infected with either wt or mutant Δ*ICP35* at an MOI of 0.1 PFU per cell and harvested at various time p.i. Progeny virus titers were determined in 35J cells (A) and Vero cells (B). Symbols: ■, wt yields in Vero cells; ◇, wt yields in 35J cells; ⊡, Δ*ICP35* yields in Vero cells; ◆, Δ*ICP35* yields in 35J cells.

0.1 PFU per cell, and harvested at various times p.i. Progeny virus titers were determined on 35J cells for virus yield (Fig. 4A) and on Vero cells for determination of reversion frequency (Fig. 4B). The results of these experiments indicated that the Δ*ICP35* mutant was severely restricted for growth on Vero cells (Fig. 4A). The yield of Δ*ICP35*-infected Vero cells was more than 500-fold lower than that of Δ*ICP35*-infected 35J cells at 24 h p.i. and reached the level of input of virus only at 48 h p.i. (Fig. 4A). To ensure that this low level of replication represents Δ*ICP35* progeny and not revertants, we also determined titers of identical samples on Vero cells (Fig. 4B). Less than 1% of the progeny virus from Δ*ICP35*-infected Vero cells at 24 h p.i. formed plaques on Vero cells (compare Fig. 4A and B). The small amounts of wt virus detected in mutant stocks are the results of homologous recombination between the Δ*ICP35* DNA and wt ICP35 DNA resident in the 35J cell line. To explore this further, we passaged the mutant virus on Vero cells and determined the titer of progeny virus. A decrease in the 35J/Vero ratio was observed, indicating the increased occurrence of revertants. This was also confirmed by the reappearance of ICP35 as examined by Western blotting (results not shown). We conclude, therefore, that the full-length ICP35 is important but not essential for viral growth in cell culture.

TABLE 2. Effect of MOI of wt and Δ*ICP35* on Vero cells[a]

Virus	MOI	Viral yield (burst size)[b]		Ratio of burst size (35J/Vero)
		Vero	35J	
KOS	5.0	1.3×10^8 (87)	1.3×10^8 (59)	0.68
	1.0	3.3×10^8 (220)	1.0×10^8 (45)	0.21
	0.1	2.5×10^8 (170)	2.2×10^8 (100)	0.59
Δ*ICP35*	5.0	9.0×10^5 (0.6)	6.2×10^7 (28)	47
	1.0	6.0×10^5 (0.4)	9.0×10^7 (45)	103
	0.1	8.4×10^4 (0.056)	6.2×10^7 (28)	500

[a] T25 flasks of Vero and 35J cells were infected at the MOIs indicated at 37°C and harvested at 24 h p.i. Virus yield was determined by plaque assay on 35J cells.
[b] Burst size (PFU per cell) was calculated on the basis of 1.5×10^6 Vero cells and 2.2×10^6 35J cells per flask.

To determine whether MOI affects the yield of Δ*ICP35* virus, we infected Vero cells with wt or mutant virus at MOIs of 5, 1, and 0.1 and determined the titer of progeny virus (24 h p.i) on both 35J cells (Table 2) and Vero cells (results not shown). The defect of Δ*ICP35* growth on Vero cells appeared to be more severe at low MOI. The ratio of the burst size on 35J cells to the burst size on Vero cells is approximately 50:1 to 100:1 at MOIs of 5 and 1 but 500:1 at an MOI of 0.1.

(iii) Analysis of viral DNA. We then examined the phenotype of Δ*ICP35* with regard to replication and the processing of viral DNA. Total DNA was isolated from mock-, wt-, or Δ*ICP35*-infected Vero or 35J cells at 16 h after infection. Equal amounts of DNA were digested with *Bam*HI and hybridized with ^{32}P-labeled HSV-1 *Bam*HI-K junction fragment (Fig. 5). wt amounts of mutant Δ*ICP35* *Bam*HI-K were

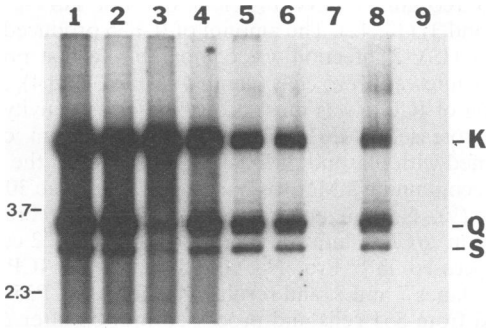

FIG. 5. Ability of the Δ*ICP35* mutant to process viral DNA. Vero cells or 35J cells were mock infected or infected with wt HSV-1 or Δ*ICP35*, and total DNA (lanes 1 to 4) and DNase I-treated DNA (lanes 5 to 9) were prepared at 16 h p.i. as described in Materials and Methods. An equal amount of DNA sample was digested with *Bam*HI, separated on a 0.8% agarose gel, blotted onto a nylon membrane, and hybridized to ^{32}P-labeled *Bam*HI-K junction fragment. Lanes: 1 and 5, wt-infected Vero cells; 2 and 6, wt-infected 35J cells; 3 and 7, Δ*ICP35*-infected Vero cells; lanes 4 and 8, Δ*ICP35*-infected 35J cells. Viral DNA isolated from Δ*ICP35*-infected Vero cells at 16 h p.i. in the presence of phosphonoacetic acid was treated as same as others. K, Q, and S, HSV-1 genome *Bam*HI restriction fragments. The locations of molecular size markers in kilodaltons are shown at the left.

detected in infected Vero cells (Fig. 5, compare lanes 1 and 3), indicating that similar amounts of wt and mutant DNA were synthesized. The ^{32}P-labeled *Bam*HI-K junction fragment hybridized not only to the junction fragment *Bam*HI-K but also to *Bam*HI-S and *Bam*HI-Q end fragments, indicating that viral DNA was processed into unit-length molecules in wt-infected Vero cells (lane 1). However, only a very small portion of replicated viral DNA was processed into unit-length molecules in Δ*ICP35*-infected Vero cells (lane 3). This defect was restored in Δ*ICP35*-infected complementing 35J cells (lane 4). To confirm these results, we also analyzed DNase I-treated samples from wt- and Δ*ICP35*-infected cells (lanes 5 through 9). As a control for the detection of input viral DNA, mutant viral DNA isolated from infected Vero cells in the presence of a specific HSV DNA synthesis inhibitor, sodium phosphonoacetate, was used (lane 9). DNase I-resistant *Bam*HI fragments K, S, and Q were detected in wt-infected Vero and 35J cells as well as in Δ*ICP35*-infected 35J cells (lanes 5, 6, and 8), but only a small amount of viral DNA was detected in Δ*ICP35*-infected Vero cells (lane 7), suggesting that a limited portion of Δ*ICP35* viral DNA concatemers was encapsidated. To quantitate these results, the intensity of radioactivity hybridizing to the *Bam*HI S fragments in DNase-I treated samples were scanned, and the relative amounts of HSV-1 DNA in each sample were determined. In this particular experiment, the amount of Δ*ICP35* DNA encapsidated in Vero cells was about 7% of the amount of wt DNA. From these experiments, we concluded that (i) mutant viral DNA replication proceeded at the wt level but only a small portion of the replicated mutant DNA was processed to the unit-length size and encapsidated and that (ii) cleavage is required for DNA encapsidation.

(iv) Electron-microscopic studies. Thin sections of virus-infected cells were examined by electron microscopy to determine whether viral mutant Δ*ICP35* formed capsids when grown in nonpermissive cells. Vero and 35J cells were infected with wt or Δ*ICP35*, harvested, fixed with 2.5% glutaraldehyde at 16 h p.i, and prepared for electron microscopy as described in Materials and Methods. Cells infected with wt HSV-1 were found to contain the three expected capsid types, A, B, and C capsids (Fig. 6A). One characteristic of B capsids is that they contain an inner core. Δ*ICP35*-infected cells were also found to contain capsids, but the majority lacked the core and were of the electron-transparent (A capsid) type (Fig. 6B). Although very few dense-cored C capsids were observed, they were not evident in this field. Our results demonstrate that capsid structures were formed in the absence of full-length ICP35.

(v) Sucrose sedimentation analysis. An alternative way to study the formation of capsid structures is to examine mutant-infected cell lysates in sucrose density gradients (12). Nuclear extracts from wt- or Δ*ICP35*-infected cells were subjected to centrifugation through 20 to 50% sucrose gradients, and fractions were collected. The first 18 of 24 total fractions were subjected to SDS-PAGE and analyzed by Western blotting with MAb MCA406 specific for ICP35 (Fig. 7). The Western blot showed that only Nb and ICP35 e,f were observed in fractions 11 to 17 of wt-infected cell lysates (Fig. 7A, lanes 12 to 18). N_0, the catalytic domain of the protease, was also detected in the same fractions as Nb and ICP35 e,f when the polyclonal antiserum specific for N_0 was used (results not shown). This is in agreement with published data in which only processed forms of the protease (N_0 and Nb) and ICP35 e,f are associated with B capsids (3, 12, 43). In contrast, no ICP35 e,f was detected in Δ*ICP35*-infected Vero cell lysates and only Nb was detected in fractions corresponding to the position of wt B capsids (Fig. 7B, lanes 9 through 14). Notably, the 20-kDa protein detected in Δ*ICP35*-infected cells was not associated with capsid structures (Fig. 3B, lane 5).

(vi) Cellular distribution and conformation of VP5 in Δ*ICP35*-infected Vero cells. We recently reported that assembly of VP5, the major capsid protein, into capsids was affected and that reactivity with conformation-dependent MAbs 8F5 and 5C, but not 3B (41), was dramatically reduced in the HSV-1 protease mutant-infected cells (9). Three-dimensional image reconstruction and the cryoelectron microscopy experiments suggested that MAbs 8F5 and 5C specifically recognize hexons of B capsids and 3B recognizes pentons of B capsids (41). To determine whether assembly of VP5 was altered in the absence of ICP35, we also tested the ability of these MAbs to recognize VP5 in Δ*ICP35*-infected Vero cells.

Vero cells were infected with either wt or Δ*ICP35* at an MOI of 20 PFU per cell and stained at 6 h p.i. with VP5 MAb 8F5 or 3B. VP5 appeared to accumulate in wt-infected cell nuclei when MAb 8F5 was used (Fig. 8B). In contrast, only some cells (1 to 3%) could be recognized by MAb 8F5 in Δ*ICP35*-infected cells, but reactivity was reduced (Fig. 8C). It was necessary to double the exposure time for Fig. 8C in order to clearly show positive reactivity. This would suggest, in agreement with the mutant viral DNA encapsidation results from the DNase I digestion experiment, that only a small portion of VP5 was correctly assembled in the observed capsids and that they all localized in the infected-cell nucleus. Reactivity to MAb 8F5 was restored in mutant-infected 35J cells (Fig. 8D). When MAb 3B was used, VP5 showed a nuclear staining pattern in wt-infected cells (Fig. 8F). However, VP5 lost its ability to localize into the nucleus and showed approximately equal intensity of both cytoplasmic and nuclear staining in Δ*ICP35*-infected cells (Fig. 8G). In mutant-infected 35J cells, VP5 relocalized into the nucleus (Fig. 8H). These findings suggest that (i) 3B recognized both cytoplasmic and nuclear VP5 and (ii) ICP35 has a novel function which is involved, directly or indirectly, in the nuclear transport of VP5.

DISCUSSION

We and others have previously demonstrated that the HSV-1 protease encoded by the UL26 gene is essential for viral growth (9, 33, 34). One would assume that the substrate of the protease, ICP35, should also be required for viral growth. The striking characteristic of Δ*ICP35* from this report was that in the absence of full-length ICP35, a small portion of replicated mutant Δ*ICP35* DNA was encapsidated and mutant progeny virus were produced. The growth ability of the mutant was significantly restricted relative to that of wt virus, as reflected by its extremely small plaque size and by a titer that was 100- to 1,000-fold lower than that of wt virus. Consistent with its small plaque size, its burst size was 50- to 500-fold lower than that of wt virus. However, the reduced burst size did not reflect a delay in the production of progeny virus by the mutant, because no significant increase in viral yield was observed even at 48 h p.i. The slight increase in infectious virus (Fig 4A) at 48 h is most probably due to complementation of growth of Δ*ICP35* by revertants since the titer of revertants on Vero cells also increased slightly at 48 h (Fig. 4B).

Since a 20-kDa protein was observed only in Δ*ICP35*-infected cell extracts, we could not rule out the possibility that this truncated protein retains some residual functions of ICP35 and is responsible for its phenotype. However, its low abundance in infected-cell extracts and our inability to detect it in capsid structures suggest that it is not performing the function of intact ICP35. In addition, the 20-kDa protein did not appear to interfere with the functions of wt ICP35, because Δ*ICP35*

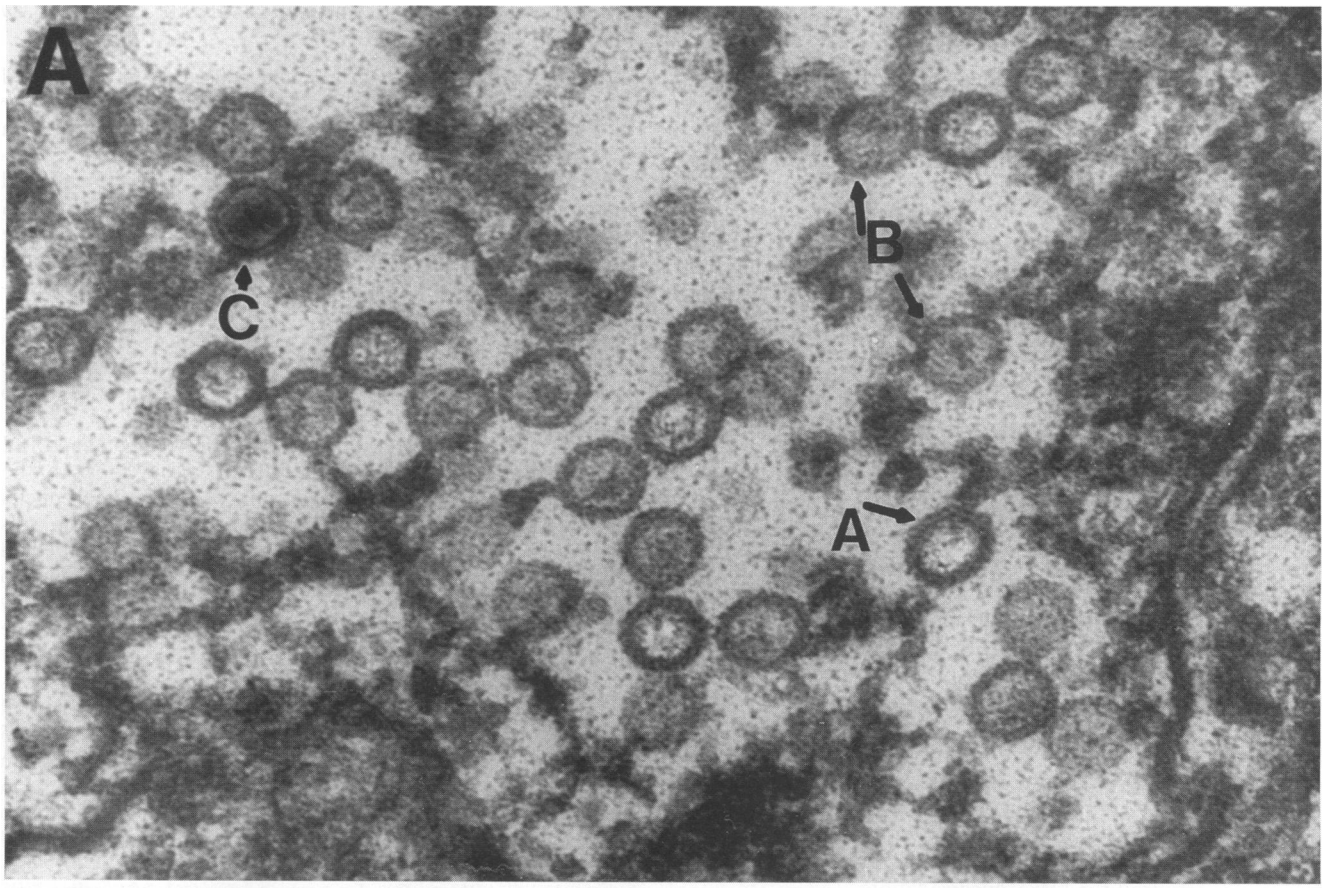
A
B
C
A

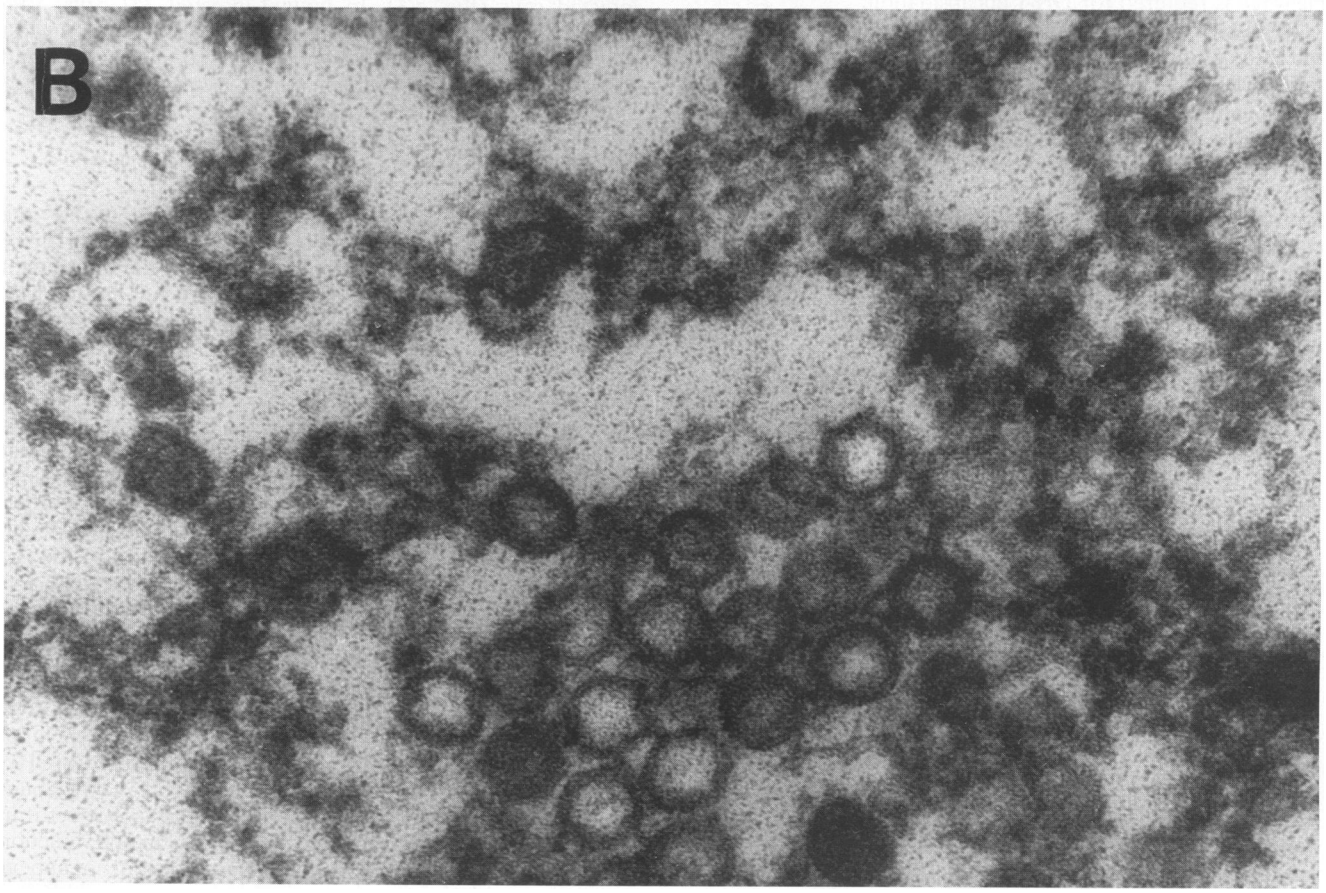
B

FIG. 6. Electron micrographs of thin sections of wt- and Δ*ICP35*-infected cells. Vero cells were infected with wt or Δ*ICP35* virus at an MOI of 10 PFU per cell. The cells were fixed and prepared at 16 h p.i. as described in Materials and Methods. (A) wt-infected Vero cells; (B) Δ*ICP35*-infected Vero cells. Magnifications, ×100,000. A, B, and C capsids are indicated in panel A.

mutant virus grew normally in 35J cells. Nevertheless, in this report we have clearly demonstrated that full-length ICP35 is not essential in tissue culture, although the growth of Δ*ICP35* mutant on nonpermissive cells was severely restricted.

The growth properties of mutant Δ*ICP35* are not unique for ICP35. It has been reported that mutations in certain genes, such as the ICP0 (37) and alkaline nuclease (39, 46) genes, cause similar growth properties. In both cases, mutant viruses were severely compromised when grown in nonpermissive cells, but a limited amount of infectious progeny virus was produced in the absence of ICP0 or alkaline nuclease. Like Δ*ICP35*, both ICP0 and alkaline nuclease mutants displayed more severe defects at low MOI (37, 39, 46). The role of ICP0 in the HSV-1 life cycle is unclear, but its functions could be partially substituted by a cell factor(s) during certain stages of the cell cycle (4).

One obvious model to explain why ICP35 is not essential is that the defect of mutant Δ*ICP35* can be compensated by Na (VP21). Na, one of the autoproteolytic products of HSV-1 protease, contains the entire ICP35 sequence within its C-terminal 329 residues (Fig. 1A). The fact that the growth of mutant Δ*ICP35* was improved at higher MOIs would suggest that Na may substitute for ICP35 functions. Results from our laboratory and others have indicated that capsid structures could be formed in the absence of Na (9, 33, 34, 37). In the present study, we also demonstrated that capsid structures could be observed in the absence of full-length ICP35 (VP22a). However, no capsid structures were detected in the absence of both Na and ICP35 (32). These results would further support the model that Na may substitute for ICP35 during the formation of capsids under certain conditions.

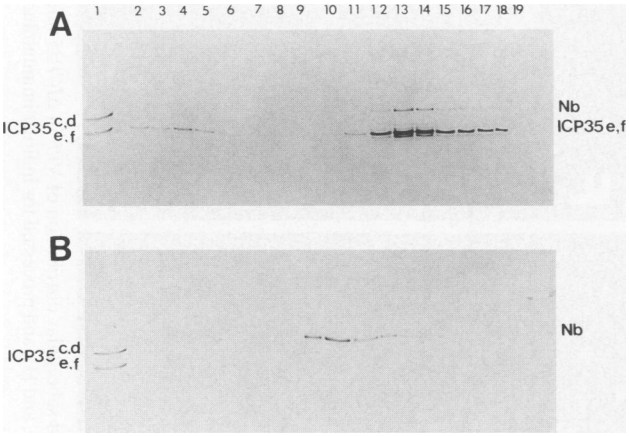

FIG. 7. Sucrose gradient analysis of nuclear lysates from infected Vero cells. Vero cells were infected with either wt (A) or Δ*ICP35* (B) at an MOI of 10 PFU per cells for 16 h. Nuclear extracts were prepared, layered onto a 20 to 50% sucrose gradient, and centrifuged at 25,000 rpm for 1 h in a Beckman SW41 rotor. Fractions were collected, and proteins from fractions 1 to 18 were subjected to SDS-PAGE (lanes 2 to 19). After the transfer, the nitrocellulose filter was probed with MAb MCA406 specific for ICP35 (9, 42). The sedimentation direction is from left to right. Lane 1 contains wt-infected cells used as markers for ICP35 c to f.

Another interesting question raised from the growth phenotype of Δ*ICP35* mutant on nonpermissive cells is whether there is another substrate besides ICP35 for the viral protease and whether that substrate, rather than ICP35, is essential for viral growth. At present, we do not have any evidence to support or refute this hypothesis.

We recently reported that structure of the major capsid protein VP5 was conformationally altered in the HSV-1 protease mutant (*m*100)-infected cells (9). The reactivity of VP5 with MAb 8F5 and 5C, but not 3B, was markedly reduced in *m*100-infected Vero cells (9). Similar but not identical results were also obtained with Δ*ICP35*-infected Vero cells. The similarity between *m*100 and Δ*ICP35* is that MAb 3B recognized VP5 in both mutant-infected cells, indicating that assembly of VP5 into capsid pentons is not altered in the absence of either the protease or full-length ICP35. One difference between these two mutants is that the reactivity of VP5 with MAb 8F5 was almost eliminated in *m*100-infected cells but could still be detected in a small portion of Δ*ICP35*-infected cells. It is unlikely that detection of VP5 with MAb 8F5 in a small portion of Δ*ICP35*-infected cells was due to wt virus contamination in the mutant stock, because MAb 5C did not recognize VP5 in any Δ*ICP35*-infected cells (11).

Whether the major capsid protein VP5 has different conformations in type A, B, and C capsids is unclear. Our previous results (9, 41) and the present study strongly suggest that VP5 displays different conformations during capsid maturation. Since MAb 3B is conformationally dependent and recognizes only native VP5 (41), our results suggest that VP5 in the absence of N_0 and Na or ICP35 and even VP5 as found in the cytoplasm is not denatured and assembly into pentons can occur in the cytoplasm. The findings that MAb 8F5 recognized nuclear VP5 in only a small portion of Δ*ICP35*-infected cells and MAb 5C did not recognize VP5 at all in Δ*ICP35*-infected cells (11) indicate that at least two different conformations are involved in assembly of VP5 into hexons. Three-dimensional reconstruction of mutant Δ*ICP35* capsids may address these differences in VP5 conformations from wt B capsids.

Because VP5 was recognized by MAb 8F5 in only small a portion of Δ*ICP35*-infected cells, the question remains whether hexons were assembled correctly in a small portion of mutant-infected cells or whether assembly of hexons was altered in all of the mutant-infected cells, with only a few recognized by MAb 8F5. We favor the latter hypothesis for two reasons. First, on the basis of the more severe phenotype of *m*100 versus Δ*ICP35*, it is conceivable that VP5 conformational alteration in Δ*ICP35*-infected cells is not as severe as in *m*100-infected cells; and, second, some of the Δ*ICP35*-infected cells showed reduced but detectable levels of VP5 (Fig. 8C). The reactivity of VP5 with MAb 8F5 in most of the mutant-infected cells could simply be below the level of detection. Since an MOI of 20 PFU per cell was used to infect cells for immunofluorescence, it is possible that few cells were infected with higher MOIs than the others and that more Na was produced to substitute functions of ICP35 in these cells.

If the major capsid protein VP5 has different conformations during capsid maturation, determination of the conformation is most probably dependent on its interactions with other viral capsid proteins. In this report, we demonstrate that ICP35 is

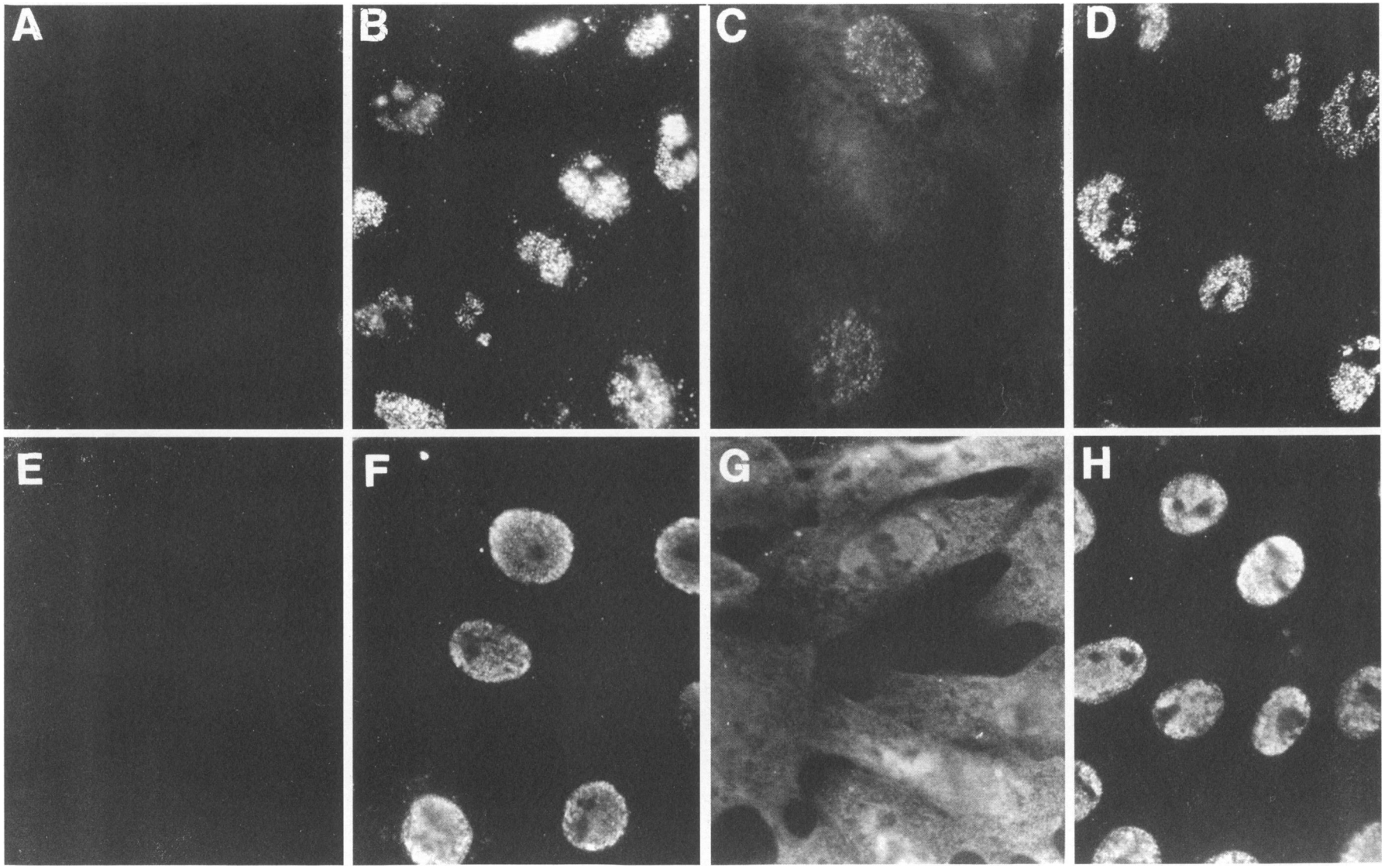

FIG. 8. Recognition and subcellular distribution of VP5 in Δ*ICP35*-infected cells. Vero cells (A, B, C, E, F and G) or 35J (D and H) were either mock infected (A and E) or infected with wt (B and F) or Δ*ICP35* (C, D, G, and H), and processed for indirect immunofluorescence at 6 h p.i. Cells were fixed, permeabilized, and incubated with anti-VP5 MAb 8F5 (A through D) or 3B (E through H).

involved in the nuclear transport of the major capsid protein VP5. The inability of VP5 to localize into the infected-cell nucleus in the absence of ICP35 could be restored when ICP35 was provided in *trans* from complementing 35J cells. These studies, however, could not distinguish whether ICP35 is directly or indirectly involved in the process of VP5 nuclear localization. After this paper was submitted, Nicholson et al. reported that VP5 was efficiently transported to the nucleus in the presence of ICP35 in coexpression experiments (28).

In recent studies, we showed that VP5 pentons localized exclusively in the nucleus of protease mutant (*m*100)-infected cells when MAb 3B was used (9). In the absence of ICP35, only a portion of VP5 localizes in the nucleus. It is likely that the 10-fold-higher expression levels of ICP35 compared with the protease in wt-infected cells (27) are normally responsible for transporting VP5 into the nucleus. Partial nuclear localization of VP5 may be due to the lower levels of the protease or to other viral or cellular proteins involved in the nuclear transport of VP5. We note that the inability of VP5 to localize in the nucleus may contribute to the growth defect observed with mutant Δ*ICP35*, because VP5 is essential for viral replication (7).

One unique feature of ICP35 is its abundance in B capsids and its absence in the mature virion. It is not yet clear how ICP35 is disassociated from B capsids during the DNA packaging. Another function of ICP35 may be to ensure the process of encapsidation. DNase I experiments indicated that approximately 7% of wt levels of Δ*ICP35* DNA was encapsidated. However, yield experiments indicated that only 0.5% of wt levels of viral progeny was produced at an MOI of 5. The MOI effect could not account for the observed difference (an MOI of 10 was used for DNase I experiments). These results argue that not all of the encapsidated viral DNAs form infectious virus in the absence of ICP35. One possible role that ICP35 may have is to ensure that DNA packaging occurs in a coordinated manner in which packing is tightly coupled to loss of ICP35 from the B capsid. Future studies on capsid maturation will hopefully shed additional light on the precise role(s) of protease and ICP35 in herpesvirus maturation.

ACKNOWLEDGMENTS

We thank Stanley Person and Prashant Desai for helpful discussions. We appreciate helpful discussion with Richard J. Colonno, Ingrid C. Deckman, and Patrick J. McCann III during the course of these studies.

This work is supported in part by grant MCB-9119056 from the National Science Foundation to J.C.B.

REFERENCES

1. **Baker, T. S., W. W. Newcomb, F. O. Booy, J. C. Brown, and A. C. Steven.** 1990. Three-dimensional structures of maturable and abortive capsids of equine herpesvirus 1 from cryoelectron microscopy. J. Virol. **64**:563–573.
2. **Baum, E. Z., G. A. Bebernitz, J. D. Hulmes, V. P. Muzithras, T. R. Jones, and Y. Gluzman.** 1992. Expression and analysis of the human cytomegalovirus UL80-encoded protease: identification of autoproteolytic sites. J. Virol. **67**:497–506.
3. **Braun, D. K., B. Roizman, and L. Pereira.** 1984. Characterization of posttranslational products of herpes simplex virus gene 35 proteins binding to the surfaces of full capsids but not empty capsids. J. Virol. **49**:142–153.
4. **Cai, W., and P. S. Schaffer.** 1991. A cellular function can enhance gene expression and plating efficiency of a mutant defective in the gene for ICP0, a transactivating protein of herpes simplex virus type 1. J. Virol. **65**:4078–4090.
5. **Casjens, S., and J. King.** 1975. Virus assembly. Annu. Rev. Biochem. **44**:555–611.
6. **Deckman, I. C., M. Hagen, and P. J. McCann III.** 1992. Herpes simplex virus type 1 protease expressed in *Escherichia coli* exhibits autoprocessing and specific cleavage of the ICP35 assembly protein. J. Virol. **66**:7362–7367.
7. **Desai, P., N. A. DeLuca, J. C. Glorioso, and S. Person.** 1993. Mutations in herpes simplex virus type 1 genes encoding VP5 and VP23 abrogate capsid formation and cleavage of replicated DNA. J. Virol. **67**:1357–1364.
8. **DiIanni, C. L., D. A. Drier, I. C. Deckman, P. J. McCann III, F. Liu, B. Roizman, R. J. Colonno, and M. G. Cordingley.** 1993. Identification of the herpes simplex virus-1 protease cleavage sites. J. Biol. Chem. **268**:2048–2051.
9. **Gao, M., L. Matusick-Kumar, W. Hurlburt, S. F. DiTusa, W. W. Newcomb, J. C. Brown, P. J. McCann III, I. Deckman, and R. J. Colonno.** 1994. The protease of herpes simplex virus type 1 is essential for functional capsid formation and viral growth. J. Virol. **68**:3702–3712.
10. **Gao, M., and D. M. Knipe.** 1989. Genetic evidence for multiple nuclear function of the herpes simplex virus ICP8 DNA-binding protein. J. Virol. **63**:5258–5267.
11. **Gao, M., L. Matusick-Kumar, and W. Hurlburt.** Unpublished data.
12. **Gibson, W., and B. Roizman.** 1972. Proteins specified by herpes simplex virus. VIII. Characterization and composition of multiple capsid forms of subtypes 1 and 2. J. Virol. **10**:1044–1052.
13. **Gibson, W., and B. Roizman.** 1974. Proteins specified by herpes simplex virus. Staining and radiolabeling properties of B capsids and virion proteins in polyacrylamide gels. J. Virol. **13**:155–165.
14. **Heilman, C. J., M. Zweig, J. R. Stephenson, and B. Hampar.** 1979. Isolation of nucleocapsid proteins of herpes simplex virus type 1 and 2 possessing immunologically type specific and cross-reactive determinants. J. Virol. **29**:34–42.
15. **Holland, L. E., R. M. Sandri-Goldin, A. L. Goldin, J. C. Glorioso, and M. Levin.** 1984. Transcriptional and genetic analyses of the herpes simplex virus 1 genome: coordinate 0.29 to 0.45. J. Virol. **49**:947–959.
16. **Jacob, R. J., L. S. Morse, and B. Roizman.** 1979. Anatomy of herpes simplex virus DNA. XII. Accumulation of head-to-tail concatemers in nuclei of infected cells and their role in the generation of four isomeric arrangements of viral DNA. J. Virol. **29**:448–457.
17. **Knipe, D. M., M. P. Quinlan, and A. E. Spang.** 1982. Characterization of two conformational forms of the major DNA-binding protein encoded by herpes simplex virus 1. J. Virol. **44**:736–741.
18. **Knipe, D. M., and A. E. Spang.** 1982. Definition of a series of stages in the association of two herpesvirus proteins with the cell nucleus. J. Virol. **43**:314–324.
19. **Ladin, B. F., M. I. Blankenship, and T. Ben-Porat.** 1980. Replication of herpesvirus DNA. V. Maturation of concatemeric DNA of pseudorabies virus to genome length is related to capsid formation. J. Virol. **33**:1151–1164.
20. **Liu, F., and B. Roizman.** 1991. The promoter, transcriptional unit, and coding sequences of the herpes simplex virus 1 family 35 proteins are contained within and in frame with the UL26 open reading frame. J. Virol. **65**:206–212.
21. **Liu, F., and B. Roizman.** 1991. The herpes simplex virus 1 gene encoding a protease also contains within its coding domain the gene encoding the more abundant substrate. J. Virol. **65**:5149–5156.
22. **Liu, F., and B. Roizman.** 1992. Differentiation of multiple domains in the herpes simplex virus 1 protease encoded by the UL26 gene. Proc. Natl. Acad. Sci. **89**:2076–2080.
23. **Liu, F., and B. Roizman.** 1993. Characterization of the protease and other products of amino-terminus-proximal cleavage of the herpes simplex virus 1 U_L26 protein. J. Virol. **67**:1300–1309.
24. **McGeoch, D. J., M. A. Dalrymple, A. J. Davison, A. Dolan, M. C. Frame, D. McNab, L. J. Perry, J. E. Scott, and P. Taylor.** 1988. The complete DNA sequence of the long unique region in the genome of herpes simplex virus type 1. J. Gen. Virol. **69**:1531–1574.
25. **Newcomb, W. W., and J. C. Brown.** 1989. Use of Ar^+ plasma etching to localize structural proteins in the capsid of herpes simplex virus type 1. J. Virol. **63**:4697–4702.
26. **Newcomb, W. W., and J. C. Brown.** 1991. Structure of the herpes simplex virus capsid: effects of extraction with guanidine hydro-

chloride and partial reconstitution of extracted capsids. J. Virol. **65:**613–620.
27. **Newcomb, W. W., B. L. Trus, F. P. Booy, A. C. Steven, J. S. Wall, and J. C. Brown.** 1993. Structure of the herpes simplex virus capsid: molecular composition of the pentons and the triplexes. J. Mol. Biol. **232:**499–511.
28. **Nicholson, P., C. Addison, A. M. Cross, J. Kennard, V. G. Preston, and F. J. Rixon.** 1994. Localization of the herpes simplex virus type 1 major capsid protein VP5 to the cell nucleus requires the abundant scaffolding protein VP22a. J. Gen. Virol. **75:**1091–1099.
29. **Perdue, M. L., J. C. Cohen, M. C. Kemp, C. C. Randall, and D. J. O'Callaghan.** 1975. Characterization of three species of nucleocapsids of equine herpes virus type 1. Virology **64:**187–205.
30. **Perdue, M. L., J. C. Cohen, C. C. Randall, and D. J. O'Callaghan.** 1976. Biochemical studies on the maturation of herpesvirus nucleocapsid species. Virlogy **74:**194–208.
31. **Person, S., S. Laquerre, D. Prashant, and J. Hempel.** 1993. Herpes simplex virus type 1 capsid protein, VP21, originates within the UL26 open reading frames. J. Gen. Virol. **74:**2269–2273.
32. **Person, S., and P. Desai.** Personal communication.
33. **Preston, V. G., J. A. V. Coates, and F. J. Rixon.** 1983. Identification and characterization of a herpes simplex virus gene product required for encapsidation of virus DNA. J. Virol. **45:**1056–1064.
34. **Preston, V. G., F. J. Rixon, I. M. McDougall, M. McGregor, and M. F. Al Kobaisi.** 1992. Processing of the herpes simplex viral assembly protein ICP35 near its C-terminal end requires the product of the whole of the UL26 reading frame. Virology **186:**87–98.
35. **Quinlan, M. P., L. B. Chen, and D. M. Knipe.** 1984. The intranuclear location of a herpes simplex virus DNA-binding protein is determined by the status of viral DNA replication. Cell **36:**857–868.
36. **Rixon, F. J., A. M. Cross, C. Addison, and V. G. Preston.** 1988. The products of herpes simplex virus type 1 gene UL26 which are involved in DNA packaging are strongly associated with empty but not with full capsids. J. Gen. Virol. **69:**2879–2891.
37. **Sacks, W. R., and P. A. Schaffer.** 1987. Deletion mutants in the gene encoding encoding the herpes simplex virus type 1 immediate-early protein ICP0 exhibit impaired growth in cell culture. J. Virol. **61:**829–839.
38. **Schrag, J. D., B. V. V. Prasad, F. J. Rixon, and W. Chiu.** 1989. Three-dimensional structure of the HSV-1 nucleocapsid. Cell **56:**651–660.
39. **Shao, L., L. M. Rapp, and S. K. Weller.** 1993. Herpes simplex virus 1 alkaline nuclease is required for efficient egress of capsids from the nucleus. Virology **196:**146–162.
40. **Southern, P. J., and P. Berg.** 1982. Transformation of mammalian cells to antibiotic resistance with a bacterial gene under control of the SV40 early region promoter. J. Mol. Appl. Genet. **1:**327–341.
41. **Trus, B. L., W. W. Newcomb, F. P. Booy, J. C. Brown, and A. C. Steven.** 1992. Distinct monoclonal antibodies separately label the hexons or the pentons of herpes simplex virus capsid. Proc. Natl. Acad. Sci. USA **89:**11508–11512.
42. **Vernon, S. K., M. Ponce de Leon, G. H. Cohen, R. J. Eisenberg, and B. A. Rubin.** 1981. Morphological components of herpesvirus. III. Localization of herpes simplex virus type 1 nucleocapsid polypeptides by electron microscopy. J. Gen. Virol. **54:**39–46.
43. **Weinheimer, S. P., P. J. McCann III, D. R. O'Boyle II, J. T. Stevens, B. A. Boyd, D. A. Drier, G. A. Yamanaka, C. L. DiIanni, I. C. Deckman, and M. G. Cordingley.** 1993. Autoproteolysis of herpes simplex virus type 1 protease releases an active catalytic domain found in intermediate capsid particles. J. Virol. **67:**5813–5822.
44. **Welch, A. R., L. M. McNally, M. R. T. Hall, and W. Gibson.** 1993. Herpesvirus protease: site-directed mutagenesis used to study maturational, release, and inactivation cleavage sites of precursor and to identify a possible catalytic site serine and histidine. J. Virol. **67:**7360–7372.
45. **Welch, A. R., A. S. Wood, L. M. McNally, R. J. Cotter, and W. Gibson.** 1991. A herpes maturational proteinase, assemblin: identification of its gene, putative active site domain, and cleavage site. Proc. Natl. Acad. Sci. USA **88:**10792–10796.
46. **Weller, S. K., M. R. Seghatoleslami, L. Shao, D. Rowse, and E. P. Carmichael.** 1990. The herpes simplex virus type 1 alkaline nuclease is not essential for viral DNA synthesis: isolation and characterization of a *lacZ* insertion mutant. J. Gen. Virol. **71:**2941–2952.
47. **Willdy, P., W. C. Russell, and R. W. Horne.** 1960. The morphology of herpes virus. Virology **12:**204–222.